

A SMALL-BORE HIGH-FIELD SUPERCONDUCTING QUADRUPOLE MAGNET*

D. B. Barlow, R. H. Kraus, C. T. Lobb and M. T. Menzel
 Los Alamos National Laboratory, Los Alamos, NM 87545

P. L. Walstrom
 Grumman Space Systems at Los Alamos, NM 87545

Abstract

A prototype superconducting quadrupole magnet was designed and built for use in superconducting coupled-cavity linacs where the use of permanent magnets is ruled out by consideration of trapped-flux losses. The magnet has a clear bore diameter of 1.8 cm and outside diameter of 11 cm and length of 11 cm. The magnet was operated at a temperature of 4.2 K and obtained a peak quadrupole field gradient of 320 T/m.

Introduction

Small-bore, high-field quadrupole focusing magnets are required between cavities in superconducting coupled-cavity linacs. Stray magnetic fields of only a few gauss in cavity walls before cooldown can be trapped and cause excessive rf losses during cavity operation. Fields of a few-hundred gauss, when applied to cavities after cooldown, can also cause excessive rf losses. Accordingly, the focusing magnets must have a low fringe field during operation and be capable of being turned off during cavity cooldown. Superconducting quadrupole magnets are a natural choice for the focusing elements, since they can be turned off during cavity cooldown, be designed to occupy little space, and be kept at liquid helium temperature by the refrigeration system for the superconducting cavities. Compact superconducting quadrupole magnets wound from commercially available superconducting wire can operate with field gradients of hundreds of teslas per meter in a clear bore of a few centimeters. This performance meets the needs of most superconducting coupled-cavity linac designs.

Design and Construction

The 2-D magnet codes POISSON¹ and FLUX2D² were used to optimize the geometry and design of the magnet and to calculate the expected fields and operating currents. A schematic of the prototype magnet is shown in Figs. 1 and 2. The magnet was designed to fit between cavities in a typical array of small superconducting accelerating cavities, and includes field clamps to minimize fringe fields. The magnet has a clear

bore diameter of 1.8 cm and can be assembled around a beam pipe and vacuum flange projecting from the end of a cavity without removing the flange or adding extra beam pipe between cavities. The outside dimensions of 11 cm long by 11 cm in diameter were kept as small as possible to minimize the spacing between cavities. The poles, flux-return yoke, and field clamps were all made of low-carbon steel. The 6-cm-long poles were made with flat instead of hyperbolic tips, since the poles are almost completely saturated at nominal operating fields.

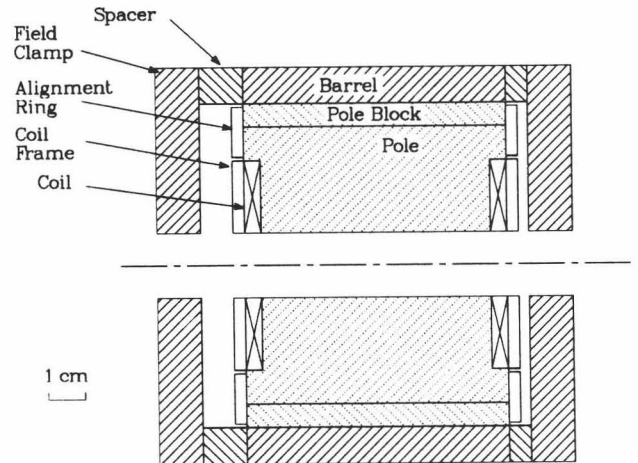


Fig. 1. Schematic of the magnet (side view).

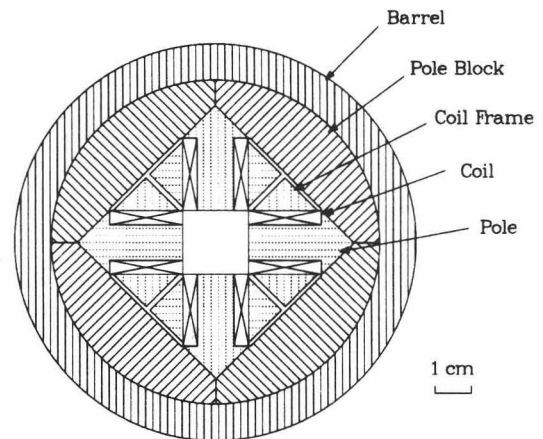


Fig. 2. Schematic of the magnet (end view).

*Work supported by the US Department of Energy, with Los Alamos National Laboratory Program Development funds.

POISSON was used to determine the width of the pole that would minimize the the first allowed ($n=6$) harmonic. A pole width of 1 cm was found to null out the $n=6$ harmonic and produce higher order fields of less than 0.02% of the quadrupole at a reference radius of 5 mm, at typical operating current densities. The 3-D code, TOSCA³, was run for the final magnet design to estimate the gradient-length product and the magnitude of the stray field beyond the ends of the magnet. These results indicated that the 1-cm-thick field clamps, which were separated from the central part of the magnet by low-permeability stainless-steel spacers on both ends, reduced the stray fields everywhere outside the magnet to less than 100 G at nominal operating currents.

The coils for the magnet were made of commercially available 0.25-mm-diameter, 54-filament NbTi/Cu superconducting wire. The racetrack-shaped coils contain 762 turns of conductor and have a rectangular cross section measuring 2.00 by 0.35 cm. The coils were wet-wound with an aluminum-oxide-filled epoxy on a slightly oversized mandrel. After the epoxy had cured, the coils were pressed off the mandrel and the inside dimension relaxed slightly to form a snug fit when mounted on the poles. The cross section of several sample coils were inspected under a microscope to check for uniform packing of the windings. Each coil was checked for internal shorts using an impedance meter to measure the coil's Q as a function of frequency. (A short would have caused the coil to have a Q value less than the nominal.) The coils were then mounted on the poles and potted with epoxy into stainless-steel frames. The frames were needed to contain the outward Lorentz forces that would cause movement of the windings and premature coil quenches. After being potted, the coils were individually tested at 4 K to be sure they operated above 70 A without quenching; this current in the coil test configuration corresponds to $\sim 95\%$ of the short-sample critical current specified by the manufacturer. After testing, the coil and pole assemblies were mounted in the barrel of the magnet, aligned and held in place by the four pole blocks that were adjusted by set screws. The alignment of the poles was fixed by means of an alignment ring mounted on both ends of the magnet. The four coils were connected in series with superconducting bus bars made of heavy-gauge copper wire wrapped with several strands of superconducting wire. All joints were soldered with indium, and care was taken to insure that the coil leads had no sharp bends or unsupported sections between the coil and the bus bars. The bus bars were routed out the side of the magnet and indium-soldered to the ends of vapor-cooled current leads.

Results

The assembled magnet was tested in a bath of atmospheric pressure liquid helium (a temperature of

~ 4.2 K). At this temperature, the maximum current obtained was 62 A. Only a few training quenches were required to bring the magnet up to the maximum current. Fig. 3 shows a plot of the peak field in the windings, calculated by FLUX2D vs the current. Included in Fig. 3 is a plot of the short-sample critical current vs field for the superconducting wire. The intersection of the two

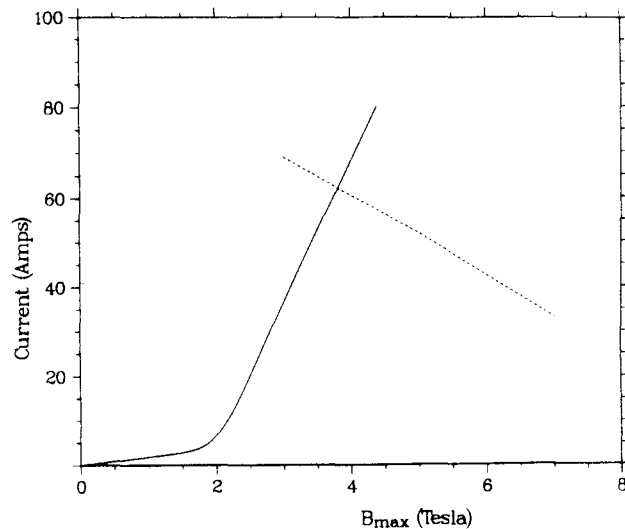


Fig. 3. Load line (solid curve) vs critical current (dashed curve) for the magnet. The calculations of the peak field in the coil windings were done using FLUX2D. The critical current vs field was provided by the manufacturer of the wire.

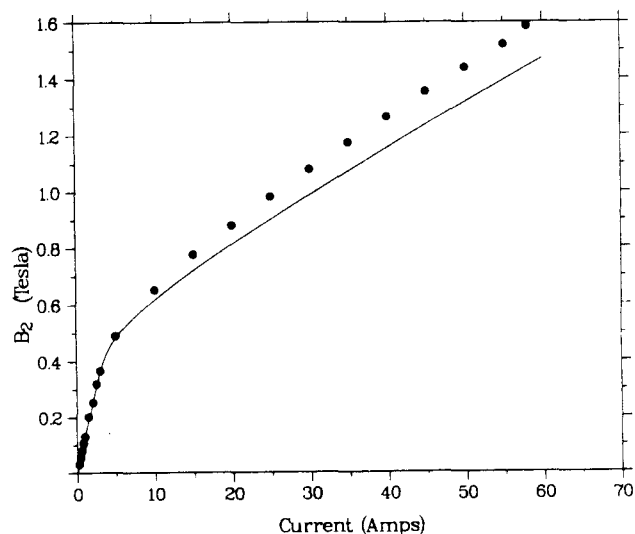


Fig. 4. The quadrupole field (B_2) at a reference radius of 5 mm measured by the Hall probe (solid points) and calculated by FLUX2D (solid curve) vs the magnet current.

curves indicates the maximum current achievable. A peak current of 62 A for the complete magnet corresponds to a field of ~ 3.7 T in the coil windings, which is $\sim 95\%$ of the short sample critical current.

The radial field near the center of the magnet was measured with a small Hall probe at a radius of 5 mm. The Hall probe could be rotated about the axis of the magnet and provided a map of the central field. The resolution of this measurement was limited by the finite size of the probe. In addition, a rotating coil was used to measure the integral field map and integral multipole strengths of the magnet. The coil consisted of 100 turns of wire wound around a rectangular form that was parallel to the magnet axis and extended beyond the fringe fields on both ends of the bore. The coil voltage was integrated by a voltage integrator and the coil angle was measured by a potentiometer to obtain the flux as a function of the angle. A plot of the quadrupole field measured by the Hall probe as a function of the magnet current is shown in Fig. 4, along with the field calculated by FLUX2D. The reason for the $\sim 10\%$ disagreement between the calculated and measured fields above 5 A is not understood. Saturation of the iron pole tips occurs at a current of 5 A, as indicated by the change in slope of this curve. At 60 A the pole-tip field was 2.88 T, corresponding to a quadrupole gradient of 320 T/m. The rotating coil measured a gradient-length product, normalized to 60 A, of 16.4 T. Fourier analysis of the rotating coil data at 55 A indicated that the integral dipole and sextupole contributions were 3% and 1%, respectively, of the quadrupole, at a radius of 7 mm. The dipole term is most likely the result of a ± 0.1 mm offset in the alignment of the rotating coil, while the sextupole term is probably the result of a slight misalignment of one or more of the coils. After operating the magnet at 60 A, the remnant fields on the surface of the magnet measured less than 1 gauss.

Summary

A working prototype superconducting quadrupole has been built and tested. The magnet achieved $\sim 95\%$ of its calculated critical current limit. At maximum current, the magnet produced a quadrupole gradient of 320 T/m and gradient-length product of 16.4 T. The small stray and remnant fields of this magnet should not interfere with the performance of nearby superconducting cavities. An estimated 25% increase in the quadrupole strength of the magnet could be achieved by operating the magnet at a reduced temperature of 1.8 K. Calculations also indicate a 10% increase in the field strength could be realized by using the rare-earth metal, holmium, as a pole material, in place of low-carbon steel. Holmium saturates at 3.9 T, vs 2.2 T for iron, and has a slightly higher permeability at fields above 4 T. In addition, the Curie temperature of holmium is 20 K, making it possible

to erase any remnant field in the poles by raising the temperature above this point.

References

1. User's Guide for the POISSON/SUPERFISH Group of Codes, LANL Report No. LA-UR-87-115, Los Alamos Accelerator Code Group, (1987).
2. Magsoft Corporation, Troy NY, USA, (1987).
3. Vector Fields Limited, Oxford England, (1988).